Structure data in ENSDF from Nuclear Reactions; and XUNDL database

Balraj Singh

Department of Physics and Astronomy

McMaster University, Hamilton, Ontario, Canada

(Includes a presentation on particle-transfer reactions by D.G. Burke at NSDD-2005)

IAEA-ICTP ENSDF Workshop, Trieste, Italy

March 24-28, 2014

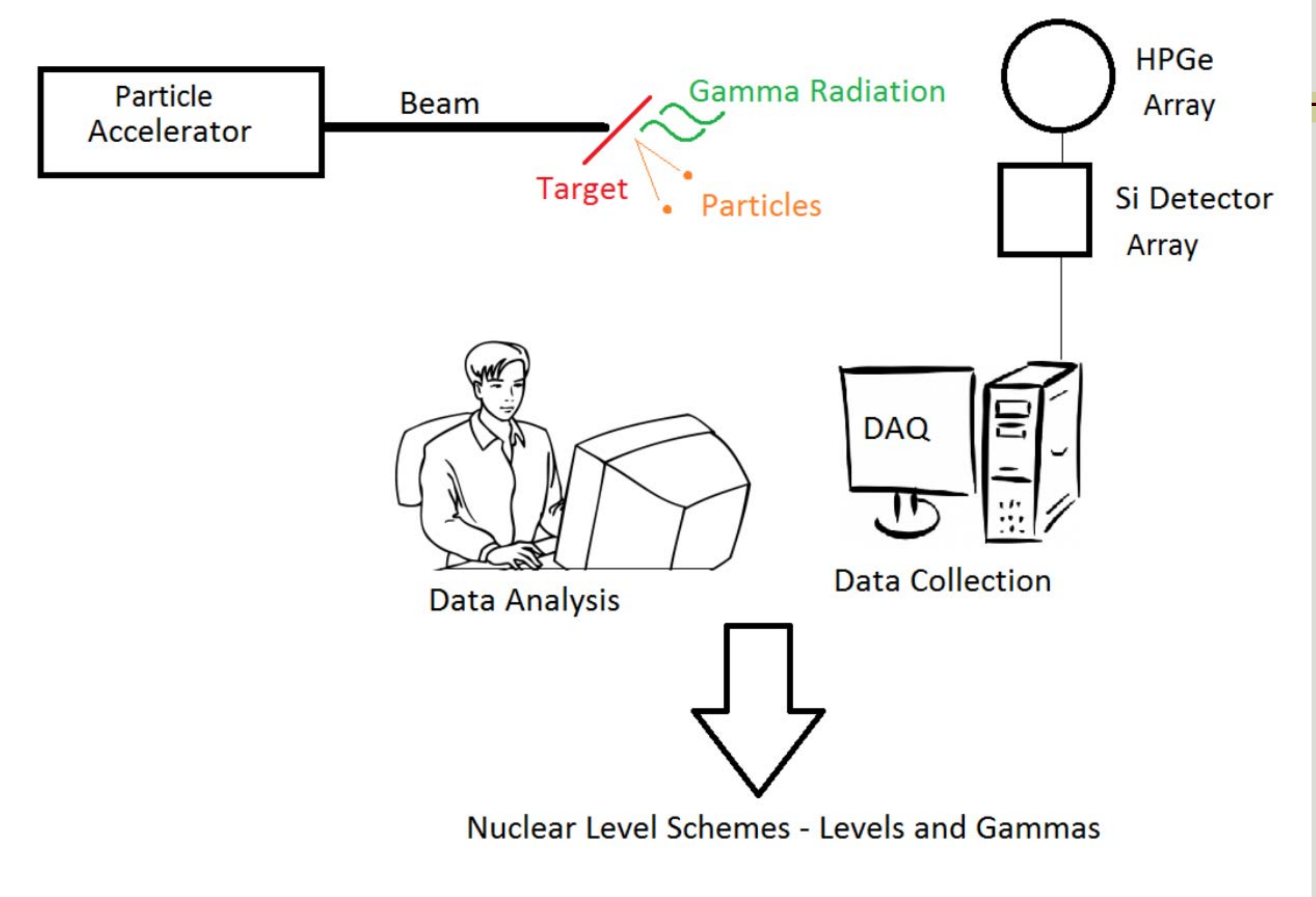
Particle Accelerator
Beam
Gamma Radiation
HPGe Array
Target
Particles
Si Detector Array
DAQ
Data Analysis
Data Collection
Nuclear Level Schemes - Levels and Gammas

Nuclear Reactions

1917: First induced nuclear reaction:

$^{14}N+\alpha \rightarrow ^{17}O+p$: Rutherford

Alpha particles from radioactive isotopes.

1932: Cockcroft and Walton: voltage multiplier

$p+ ^{7}Li \rightarrow ^{8}He^{*} \rightarrow 2\alpha$

1937-RMP: Livingstone and Bethe: about 20 levels known from reactions

Nuclear Reactions

- Bound states: various types of reactions leading to structure information for levels populated in these reactions.
- In-beam gamma-ray studies utilizing light-ion, heavy-ion, deep inelastic scattering, fusion-fission reactions, fission induced by light ions, inverse kinematic reactions for one or two nucleon knockouts, etc.: high-spin structures (Also from prompt γ in SF decay e.g. Cf-252 decay)
- Neutron, proton or alpha-particle capture followed by gamma emission: low-spin
- Coulomb excitation: light ion or heavy ion: particle and/or gamma detection: low- and high-spin levels.
- Nuclear-resonance fluorescence: low spin

Nuclear Reactions..

- Inelastic scattering such as (n,n'), (n,n'γ), (p,p'), (p,p'γ), (α,α'), etc.: low-spins: gamma and/or particle detection
- Single-particle transfer reactions such as (d,p), (d,t), etc.: low-spins: particle detection; in rare cases gamma detection.
- Two-particle transfer reactions such as (p,t), (t,p), etc.: low-spins: particle detection; rare gamma det.
- Multi-particle or cluster transfer: low- and high-spins: particle detection.
- Charge-exchange reactions such as (p,n), (^{3}He,t), etc. : low-spins: particle detection

Nuclear Reactions

- Unbound states (resonances): according to recently revised ENSDF policies, inclusion of levels, widths and gamma data for charged-particle resonances (proton, alpha, etc.) is required. Reactions: (p,p), (p,γ), (α, γ), etc. : low-spin. Particle and/or gamma detection.
- E(level) – deduce from S(P)+E(P)(c.m.), where E(p)(c.m.) is deduced from measured E(P) (lab)
- Neutron resonances: (n,γ), (n,n): low-spin: neutron and/or gamma detection. Requirement when final levels are bound, optional otherwise.

Quantities given in ENSDF
LEVELS

Energies: from particle-spectrum or excitation function or from measured gamma-ray energies and level scheme based on coincidence data (GTOL)

- $J\pi$ and T (or T_z) : spin, parity, isospin
- Half-lives: method cited e.g. delayed-gamma, DSAM, RDDS, etc. ($T_{1/2}$ given not mean lifetime in ENSDF)
- $B(E\lambda)$, $B(M\ \lambda)$ – transition probabilities e.g. from Coulomb Excitation or NRF
- L : orbital angular momentum transfer
- S or C^2S: spectroscopic factors. (Cross section data in comments-optional).
- g factor, μ and Q: static magnetic dipole and quadrupole moments: generally for g.s. and isomers. (Transition quadrupole moments in comments)
- Decay modes for g.s. and isomers.
- β_2, β_3, β_4 - deformation parameters deduced from experimental data
- Γ, Γ_i – total and/or partial widths: generally for resonances (or PDR)
- Resonance energies: generally in lab system
- Configurations and/or band structures, band crossings, etc.:

Quantities given in ENSDF
GAMMAS

- E_γ - measured gamma-ray energy (without recoil correction)
- Iγ - measured relative intensity or branching ratio
- Multipolarity (Mult) and multipole mixing ratio (δ) (Krane-Steffen convention)
- Theoretical conversion coefficient (from BrIcc code) for assigned Mult and mixing ratio.

  (Transitions with E0 admixture or pure E0 need to be handled with care)

  Transition intensity: I(γ+ce): if available or needed.

  γ-γ coincidence evidence: character "C" in column 78 in data file.
- In support of Mult and δ: (information in comments or data-continuation records)
- Measured electron conversion data such as K-, L-shell conversion coefficients, sub-shell ratios (L1/L2/L3..)

  Measured angular distribution/correlation coefficients (A_2, A_4); DCO ratios, Angular asymmetry ratios, Linear polarization coefficients.

  B(Eλ), B(Mλ) – transition probabilities (generally in W.u.)

Nuclear reactions

- To investigate Nuclear shapes, shape co-existence, n-p interaction by experimentally observing nuclear rotational bands with normal deformation, superdeformation and octupole deformation, role of γ deformation and triaxiality, magnetic rotational bands, chirality, signature splitting, backbending, wobbling rotational modes, ….
- Comparison of observed structures with theoretical calculations based on: Cranked Nilsson-Strutinski shell model; Routhians surface contours, large-scale shell-model for low-mass nuclei, IBA model, etc.

High-spin studies

Since paper by Morinaga and Gugelot: NP 46, 210 (1963), such data continue to form a large structure data bank in ENSDF. Still a fairly major effort.

- Reactions with light ions (p, d, t, ^{3}He, ^{4}He): J<12
- By heavy-ions (A>4): Fusion-evaporation reactions:

  J up to 68 and 70.5. Mostly neutron-deficient nuclei.
- Deep inelastic reactions; one- or two-nucleon knockout reactions in inverse kinematics. (Recent experiments with RI beams). Investigation of *Terra Incognita* (neutron-rich region)
- Since mid-eighties, large gamma-ray detector arrays: Gammasphere, Eurogam, GASP, SeGA, EXOGAM, GRIFFIN, MINIBALL, INGA, , etc. New and more powerful and versatile arrays: GRETA, AGATA. Clovers, Clusters, Segmented HPGe detectors. These are often coupled to particle detection arrays such as MINIBALL, ISIS, etc., and Neutron detectors such as Neutron Wall, MoNA, Magnetic spectrometers for conversion electrons

What is measured

- E_γ , $I\gamma$, $\gamma\gamma$-coin , (charged particle, neutrons, ER) γ-coincidences
- α, α_K, … - internal conversion coefficients, usually from $I(ce)/I\gamma$; sometimes from intensity balance (note: this gives α_{exp}).
- K/L, L1/ L3 … - ce sub-shell ratios
- A_2, A_4 … - Legendre polynomial coefficients characterizing angular distribution ($\gamma(\theta)$) or angular correlation ($\gamma\gamma(\theta)$).
- DCO ratio – directional correlation of gammas from oriented nuclei.
- ADO asymmetry ratio - *e.g.*, $I\gamma(\theta_1)/I\gamma(\theta_2)$
- Linear polarization: polarization asymmetry or IPDCO ratios
- Level $T_{1/2}$ – from $\gamma(t)$, DSAM, RDM, centroid-shift, delayed coincidence, *etc*., if measured in that reaction (state method used).
- g-factor – include if measured in that reaction
- Quite often details of data from high-spin studies are missing in publications; need to request authors.

What quantities are deduced

- Level energy, spin, parity, lifetime, magnetic moment, transition quadrupole moment, B(M1)/B(E2) or some other reduced transition probability ratios.
- Spins and parities deduced from multipolarities and mixing ratios deduced from angular distribution/correlation data.
  (Krane-Steffen convention in ENSDF for mixing ratio; opposite to Rose-Brink convention)
- Angular Distributions:
- Iγ as a function of angle θ with respect to beam direction:
  - $$\mathbf{W(\theta)=1+A_2P_2(\cos\theta)+A_4P_4(\cos\theta)+ \ldots}$$

  A_2, A_4 as signed values included in ENSDF
- A_2, A_4 … depend on ΔJ, mixing ratio and degree of alignment σ/J, where σ is half-width of Gaussian describing the magnetic substate population.
- For high-spin states, W(θ) is largely independent of J.
- Alignment is reduced or absent if level lifetime is long e.g. micro-sec isomer.
- **W(θ) can determine ΔJ but <u>not</u> Δπ. Need other arguments for**

Angular Distributions

Typical values of A_2, A_4 for θ relative to beam direction if $\sigma/J=0.3$

ΔJ	Multipolarity	Sign of A_2	Sign of A_4	Typical A_2	Typical A_4
2	Q	+	-	+0.3	-0.1
1	D	-		-0.2	0.0
1	Q	-	+	-0.1	+0.2
1	D+Q	+ or -	+	+0.5 to -0.8	0.0 to +0.2
0	D	+		+0.35	0.0
0	Q	-	-	-0.25	-0.25
0	D+Q	+ or -	-	+0.35 to -0.25	0.0 to -0.25

Quantities deduced: DCO ratios

- **D**irectional **C**orrelations of γ-rays from **O**riented states of Nuclei
- If γ_K (known multipolarity) and γ_U (unknown multipolarity) are measured in coincidence using detectors at angles θ_1 and θ_2 relative to the beam direction:
- DCO=I(γ_U(at θ_1) gated by γ_K(at θ_2))/I(γ_U(at θ_2) gated by γ_K(at θ_1)) .
- Sensitive to ΔJ, multipolarity and mixing ratio; **independent of Δπ.**
- Gating transitions are frequently stretched quadrupole, but stretched dipole may also be used. It is necessary to state gates in a dataset
- Remember that almost similar values are expected for stretched quadrupoles and for ΔJ=0, dipole transitions (although the latter are less common).
- Also ADO ratios are commonly seen now when count rates are low.
- Once again such measurements **can determine ΔJ but not Δπ. Need other arguments for assignment of parity.**

DCO Ratios

Typical DCO values for θ_1=37°, θ_2=79°, σ/J=0.3

ΔJ_γ^{gate}, Mult	ΔJ_γ	Mult	Typical DCO
2, Q	2	Q	1.0
2, Q	1	D	0.56
2, Q	1	D+Q	0.2 to 1.3
2, Q	0	D	1.0
2, Q	0	D+Q	0.6 to 1.0
1, D	2	Q	1/0.56
1, D	1	D	1.0
1, D	0	D	1/0.56

Parity assignment

- L and $\Delta\pi$: from measured subshell ratios or conversion coefficients.
- $\Delta\pi$ may be determined by γ linear polarization measurements.
- When transition strengths can be deduced from measured level lifetimes (or estimated from coincidence resolving times) and branching known, **R**ecommended **U**pper **L**imits (RUL) can be used to rule out some multipolarities (*e.g.*, a stretched Q transition for which $B(M2)_W$ exceeds 1 can be assigned as E2). Similarly, for a D+Q transition with large mixing, RUL may reject E1+M2.
- Assign Mult when measured information indicates a clear preference for that assignment; otherwise, let $\gamma(\theta)$ or DCO data speak for themselves. (Exception: if no measurement exists but mult. is needed for some reason, use notation for assumed value: [M1+E2]
- Notes: many authors in papers assign definite MULT even when there are no data to support. In ENSDF, these should not be given
- Ordering of transitions in cascades often disagree: example Pm-139.

In-beam Gamma-ray data

- One data set for each reaction. Mixing relative intensities from different reactions in a single data set is not advised. Also separate datasets for prompt and delayed gamma data.
- Spin-parities are generally taken from original authors' assignments, but in case of differences, comparison should be made with those in Adopted dataset for a nuclide.
- Special care needed in the assignment of multipolarities. In many cases, these may be differently expressed from those given by the authors, or in some others not given at all.
- For level energies, GTOL code is used for a least-squares fit of the gamma-ray data. If reduced chi-squared is high, try to resolve the situation, sometimes by increasing uncertainties or by omitting some gamma-ray energies. GTOL also points out those gamma-ray energies which deviate from the input values. Values which differ by more than 3σ need special attention.

Particle-transfer data: no gamma-ray detection

- Stripping: (d,p), (^{4}He,^{3}He), (pol d,p), (^{3}He,d), *etc*.
- Pickup: (p,d), (d,t), (pol d,t), (^{3}He, ^{4}He), (t, ^{4}He), *etc.*
- Measurements: particle spectra from which level energies are deduced; absolute or relative differential cross sections, angular distributions and vector analyzing powers which lead to L-transfers, J, and spectroscopic factors using DWBA analysis
- $(d\sigma/d\omega(\theta))_{exp}$= $(d\sigma/d\omega(\theta))_{DWBA}$ x N x (S or C^2S'), where N=normalization factor for DWBA. C=isospin coupling coefficient S'=S (for pickup). $S'=S(2J_f+1)/(2J_i+1)$ (for stripping)
- For unpolarized beams J= L+1/2 or L-1/2, other arguments needed to assign one value
- In inverse reactions with RIB, longitudinal momentum distributions are measured together with angular distributions

Deformed Nuclides; α and lighter beams;

Fingerprint method for rotational band assignment

- $(d\sigma/d\omega(\theta))_{exp}$ / $[(d\sigma/d\omega(\theta))_{DWBA} \times 2N] = c^2(jl)\,V^2$,
- where c=is amplitude of Nilsson state wavefunction for transferred nucleon, V is fullness factor describing partial filling of target nucleus orbitals.
- Fingerprint: experimental cross section pattern for band members for a specific Nilsson configuration agrees well with that predicted by Nilsson-model wave functions, or it differs distinctly from those for other plausible configurations.
- *Example:* $(d\sigma/d\omega(60^\circ))$ (1997Bu03) for ^{226}Ra(t,α)^{225}Fr:

Orbital:	1/2[400]	1/2[530]	**1/2[541]**	3/2[402]	3/2[651]	**3/2[532]**	Expt.	Mixed
J=3/2	23	14	1.5	103	0.0	0.7	~1.5	0.9
J=5/2	7.6	0.2	13	4.6	0.03	6.2	14	10
J=7/2	0.4	39	2.0	1.2	0.0	3.3	20	4.1
J=9/2	0.05	0.4	33	0.05	2.0	26	~45	49

- Reality (not so simple!): 3/2[532] mixed with 1/2[541] fits σ, energy.

Two- and multi-particle transfers Charge-exchange reactions

- Two-particle transfer: (p,t), (t,p), (^{4}He,d), …
- Multi-particle transfer: (α,p), (^{6}Li,d) …
- Level energies, L-transfers. DWBA or coupled-channel analysis of angular distribution data.
- Jπ(level)=J(target)+L; $\pi_i\pi_f=(-1)^{Jf}$, for <u>strong</u> groups only in two-neutron, two-proton or α–particle transfer; assuming pairs of identical particles can be assumed to be transferred in relative s state for **strong** groups
- Charge-exchange reactions: (^{3}He,t), (t, ^{3}He), (d, ^{2}He), (p,n)
- Level energies, L=0 Gamow-Teller states, GT strengths: see several very recent studies at RCNP, Osaka.
- Isobaric analog state (IAS): most intense peak in spectrum

Single- and Two- Particle Transfer Reactions, Including Inverse Kinematics

D.G. Burke
Department of Physics and Astronomy McMaster University
Hamilton, Ontario, Canada
L8S 4M1

IAEA-NSDD-2005 Meeting, McMaster University
June 7, 2005

Outline

1) We consider direct single-step reactions that transfer on or two nucleons

2) What can be learned from single-nucleon transfer reactions?

   (a) Q-values and excitation energies
   (b) l -transfers
   (c) *j*-transfers (with polarized beams)
   (d) Hole or particle character (from relative pickup and stripping strengths)
   (e) Configuration identification and purity (from absolute cross sections)

3) Spectroscopic strengths – spherical and deformed nuclei – “fingerprints” and pattern recognition

4) Reactions with inverse kinematics

1. Typical experimental setup for 'traditional' light-ion reaction experiments

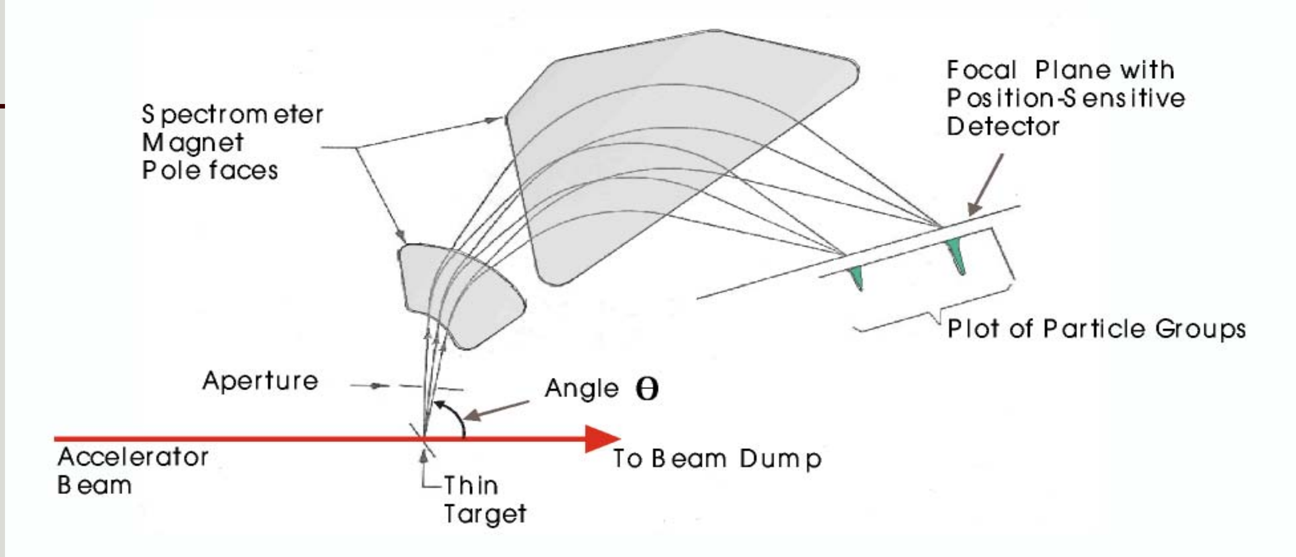

- In this case, a magnetic spectrograph is used to analyze and detect reaction products (other detectors may be used, but the good resolution of a magnet is often important).
- For good resolution, target must be very thin and most of beam goes through to 'beam dump'
- The differential cross section, $d\sigma/d\Omega$, is measured as a function of reaction angle θ
- For comments below, two very important conditions must be met:

1. The reactions must be a direct reaction: i.e., no significant compound nucleus contribution (process occurs while the projectile passes through the region of the nucleus).
2. The reaction must be a single-step process: no significant multi-step excitations such as, e.g., Coulomb excitation of target or final nucleus by the projectile or ejectile.

2. What can be learned from single-nucleon transfer experiments

(a) Reaction Q-values and excitation energies of levels – measured energies of reaction products.

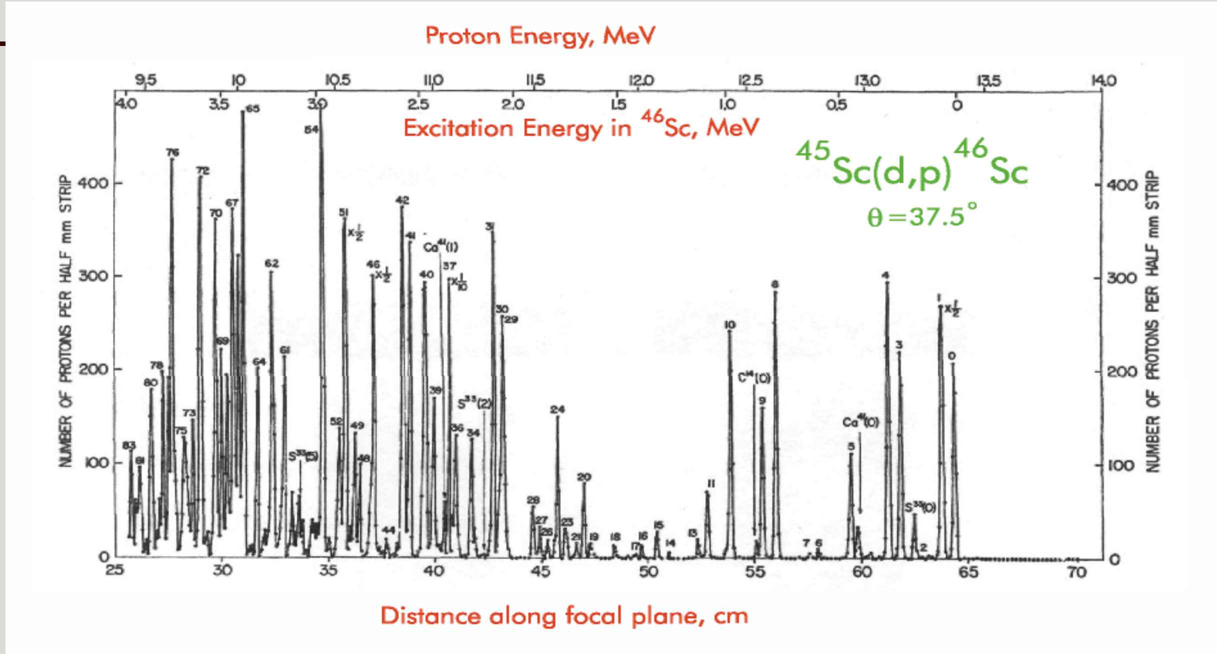

Proton spectrum from the 45Sc(d,p)46Sc reaction at 7 MeV,
by Rapaport *et al*. [Phys. Rev. **151** (1966) 939].

- Each peak represents a level in the residual nuclide.
- Measured peak position along the focal plane with known magnet calibration, gives ejectile momentum, and thus its energy. Thus, Q-values and excitation energies are obtained
- Note the high level density, even in a medium-heavy nuclide (A ~ 45), means good resolution is necessary.

2. What can be learned from single-nucleon transfer experiments *cont.*

(b) l -values for transitions – from angular distributions of cross sections.

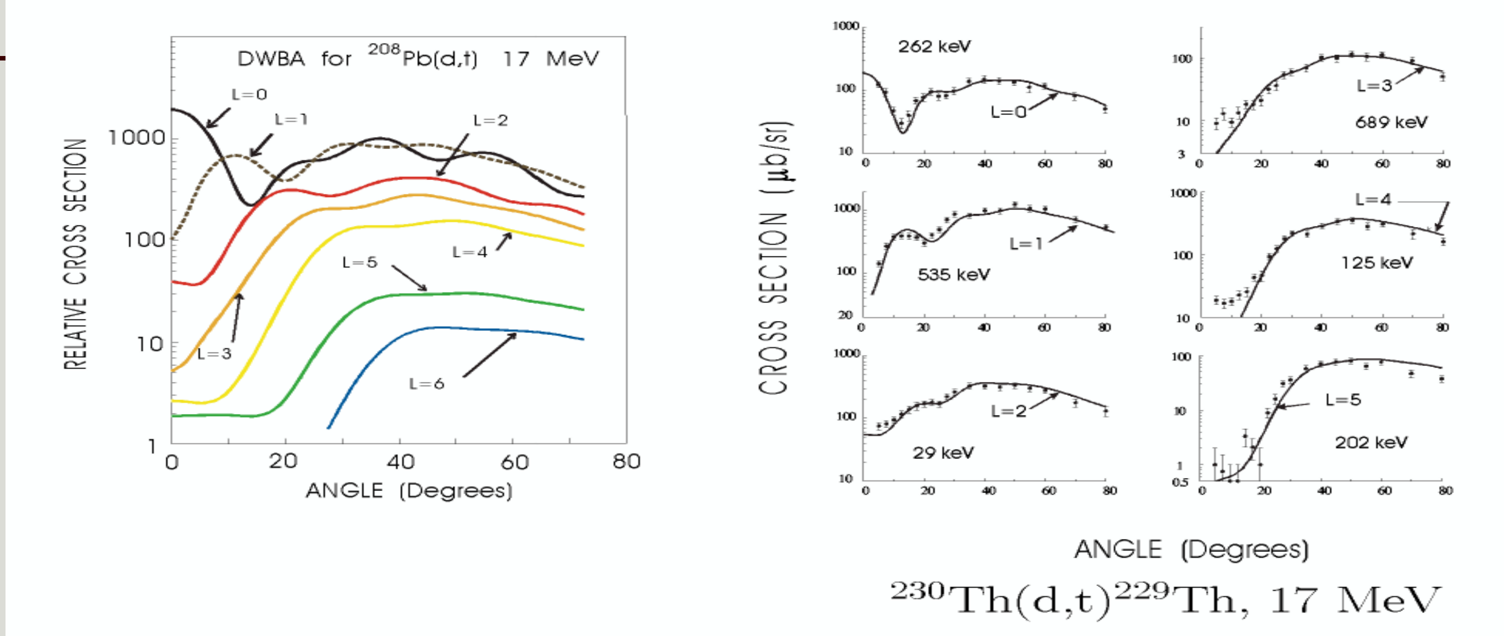

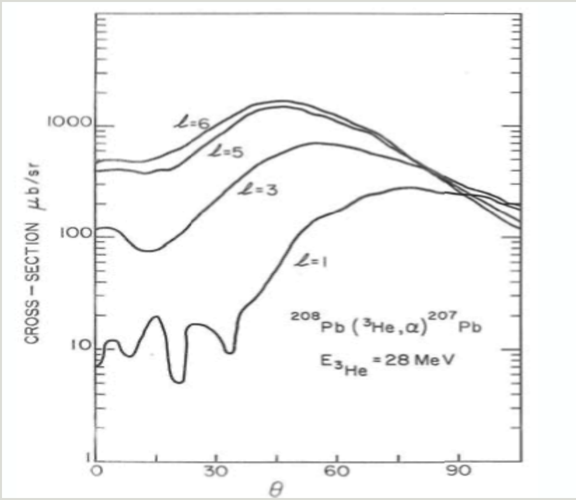

The (^{3}He,a) reaction favors higherl -values (l ~ 6), so helps locate such transitions, and the ratio of (^{3}He,a) and (d,t) cross-sections gives another indication of l -value.

2. What can be learned from single-nucleon transfer experiments *cont.*

(c) *j* - transfer in the reaction – from analyzing powers when using polarized beams

For spin 1/2 beam particles the 'Analyzing power' can be defined as

$$A_y = \frac{\left(\frac{d\sigma}{d\Omega}\right)_{\uparrow} - \left(\frac{d\sigma}{d\Omega}\right)_{\downarrow}}{\left(\frac{d\sigma}{d\Omega}\right)_{\uparrow} p_{\downarrow} + \left(\frac{d\sigma}{d\Omega}\right)_{\downarrow} p_{\uparrow}}$$

Where $\uparrow$ and $\downarrow$ indicate spin 'up' and 'down' polarizations of the beam, both perpendicular to the reaction plane (the 'p' values are degrees of polarization of the beam).

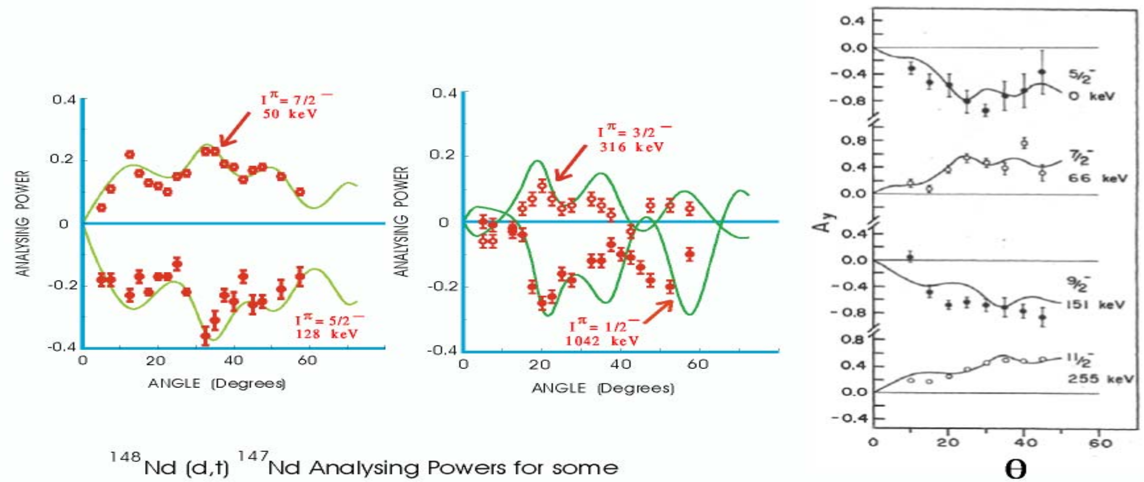

^{148}Nd (d,t) ^{147}Nd Analysing Powers for some levels with l=1 and l=3

^{154}Sm(t,α) ^{153}Pm Analysing Powers for the 5/2$^-$[532] rotational band

For each case shown, A_y is predominantly positive for levels with $j = l + 1/2$ and negative for those with $j = l - 1/2$.

3. Spectroscopic Strengths

The “spectroscopic factor”, S_l is defined by

$$\frac{d\sigma}{d\Omega} = \frac{2I_f+1}{2I_i+1}\sum_{\ell} S_\ell [N\frac{d\sigma}{d\Omega}(\theta,\ell,j)]_{DW}$$

S_l depends only on the nuclear structure.

N is effectively a normalization factor.

All the dependence on reaction kinematics, beam energy, angle, etc., is in the DWBA calculation, $d\sigma/d\Omega(\theta, l, j)]_{DW}$.

For a (d,p) reaction on an even-even target with a completely empty shell model state *j*,l which could hold 2*j* +1 nucleons, the value of S_l would be unity.

For a pickup reaction on a spherical even-even target with a full shell model state *j*,l having 2*j*+1 nucleons, S_l would be 2*j* +1.

Thus, there is a certain lack of ‘symmetry’ with this definition.

Several additional strength definitions are also used in the literature, in situations where the significance of their values is more easily seen. This has caused some frustration and confusion for NDS compilers.

e.g., for an even-even deformed target populating a rotational band member *j* , based on a pure Nilsson orbital, $\Omega^{\pi}[Nn_3\Lambda]$:

$$\frac{d\sigma}{d\Omega} = 2C^2_{j\ell}P^2[N\frac{d\sigma}{d\Omega}(\theta,\ell,j)]_{DW}$$

3. Spectroscopic Strengths *cont.*

$C_{j\ell}$ are Nilsson wave function coefficients for the transferred nucleon. P_i^2-V_i^2 for a pickup reaction and U_i^2 for a stripping reaction.

$$\text{The “Nuclear Structure Factor”} = S \equiv \frac{\frac{d\sigma}{d\Omega}}{2[N\frac{d\sigma}{d\Omega}(\theta,\ell,j)]_{DW}} \quad \text{is used.}$$

For either a stripping or pickup process, since $\Sigma_j C_{j\ell}^2=1$ for each orbital, ΣS for a band on a pure Nilsson state would be P^2. Values of S (from experiment) can readily be compared with $C_{j\ell}^2$ from model.

In contrast, Σ ‘spectroscopic factors’ could be 1/14, or 1/6 or 2!

Important Warning: In the literature there is not unanimity on which quantities are used for ‘strengths’. It is also common to use a ‘Strength’ defined as

$$S = \frac{\frac{d\sigma}{d\Omega}}{[N\frac{d\sigma}{d\Omega}(\theta,\ell,j)]_{DW}}$$

(for deformed as well as spherical nuclei) which differs by a factor of 2 from the Nuclear Structure Factor,

$$\text{Nuclear Structure Factor} = S = \frac{\frac{d\sigma}{d\Omega}}{2[N\frac{d\sigma}{d\Omega}(\theta,\ell,j)]_{DW}}$$

Also, some papers designate one or other of these quantities as C^2S where the isospin factor, C^2, should not be confused with the Nilsson coefficients, $C_{j\ell}^2$

It is necessary to look at the strength definition used in each paper before comparing results from different works!

3. Spectroscopic Strengths *cont.*

‘Fingerprints’ for deformed nuclei:

Since

$$\frac{d\sigma}{d\Omega} = 2C_{j\ell}^2 P^2 [N \frac{d\sigma}{d\Omega}(\theta, \ell, j)]_{DW}$$

The band member of spin *j* based on a particular Nilsson orbital has a cross section proportional to the C_{jl}^2 value for that orbital

Thus, each Nilsson state has a characteristic pattern of cross sections among members of its rotational band, called its ‘fingerprint’.

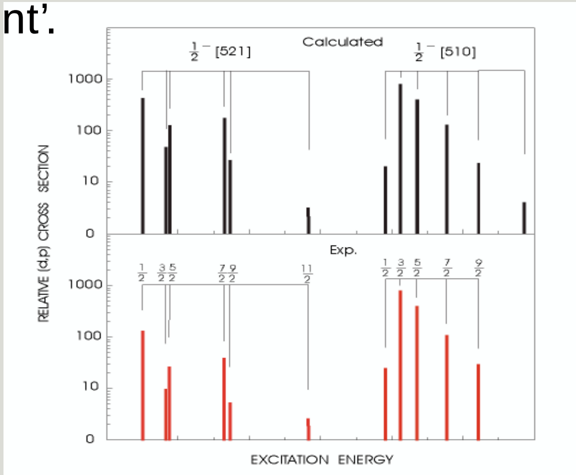

Predicted and observed (d,p) ‘fingerprints’ for two K=1/2 bands in Yb nuclei.

This example of ‘pattern recognition’ has been a very powerful tool for identifying single-proton and single-neutron configurations across a wide range of deformed nuclei.

Values of C_{jl}^2 can be nonzero for $\ell \leq N$. Thus cross sections would be zero for ℓ greater than N, i.e., for *j* greater than N+1/2

3. Spectroscopic Strengths *cont.*

In some experiments the difference between target and residual nuclides may be the same as for a single-nucleon transfer, but the conditions for a direct single-step process may not have been met.

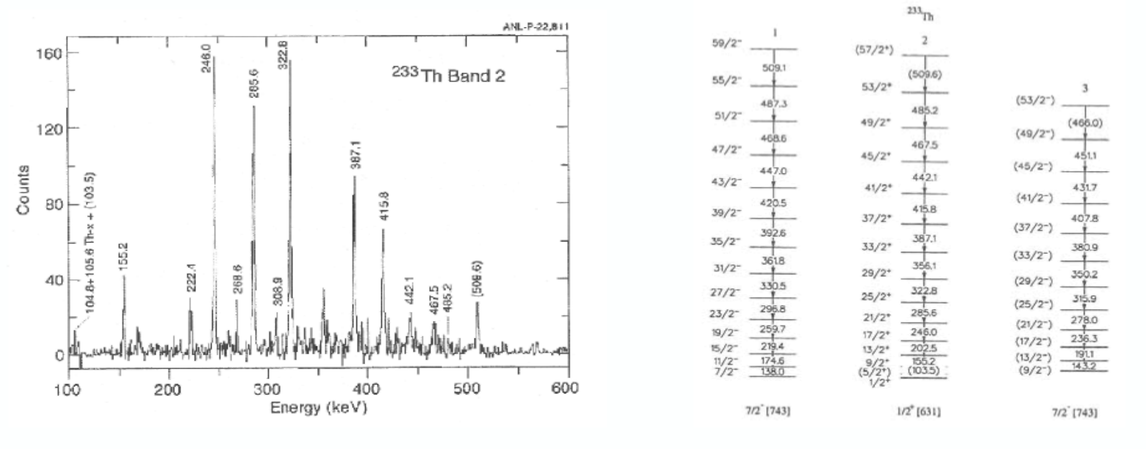

From K. Abu Saleem, Thesis, Illinois Inst. of Tech., 2002

From K. Abu Saleem, Thesis, Illinois Inst. of Tech., 2002

Coulomb excitation of ^{232}Th with ^{209}Bi beams also showed gamma rays in neighboring nuclides, including ^{231}Th, ^{233}Th, ^{233}Pa, and ^{231}Ac.

However, these are probably not pure single-step transfer reactions. The coincidence-gated gamma spectrum and proposed level structure for ^{233}Th show strong populations for spins higher than 13/2 or 15/2, suggesting multistep processes such as inelastic excitations in the entrance and exit channels are very important in these cases.

These studies are very useful for populating levels not otherwise accessible, for locating bands and determining their alignments, etc., but it would probably not be easy to extract spectroscopic strengths for single-nucleon-transfer from these data. They more properly belong in a talk about what could be learned from high spin studies.

3. Spectroscopic Strengths *cont.*

Another useful application arises from a selection rule for single-nucleon transfer strengths:

- For an even-even final nucleus, two quasiparticle (2QP) states can be populated, but 4QP, 6QP, etc., cannot (to first order).

A single-phonon state (a superposition of 2QP components) can be populated, but not two-phonon ones (involving 4QP).

Thus, if transfer strengths indicated level has dominant 2QP configuration, any multiphonon character must be minor.

Numerous 4+ levels have been suggested as double-phonons, but many of these have almost pure 2QP nature – e.g., ^{154}Gd, ^{172}Yb, ^{178}Hf.

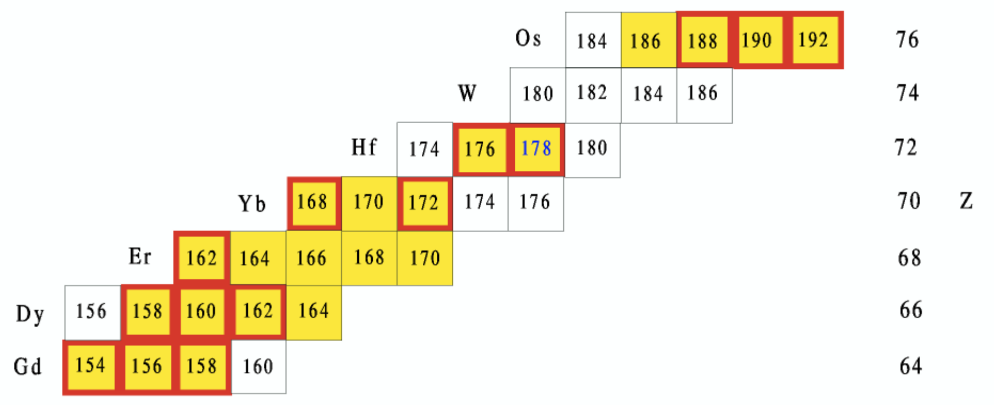

[From Proc. 10th Int. Symp. Capture Gamma-Ray Spect. (AIP, NY, 2000)p.216]

Double-phonon claims have been made for 4+ bands shaded yellow. For those with dark red outlines these claims conflict with other data.

Two-nucleon transfer reactions – (p,t) and (t,p)

Consider cases where nucleons are a time-reversed pair.

For even-even nuclei pairing correlations which lower the ground state energy also result in constructive interference of the transition amplitudes and thus a strongly-enhanced ground-state population.

L=0 transitions are readily identified experimentally by the characteristic diffraction structure in their angular distributions.

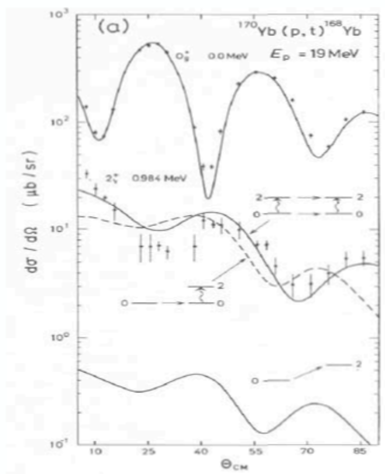

[Phys. Lett. **44B**(1973)425]

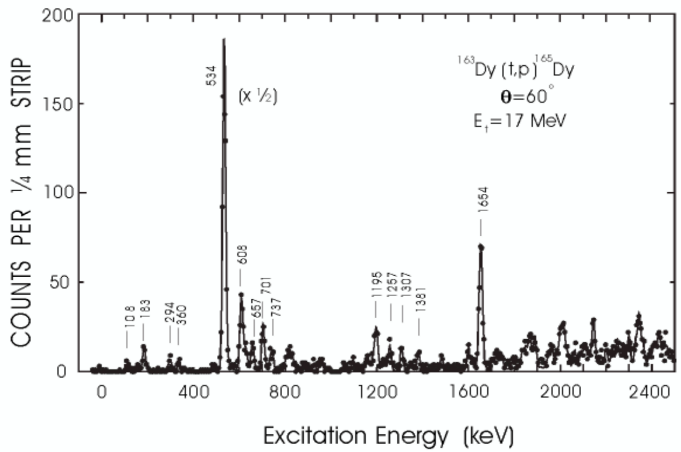

[Nucl. Phys. A **750**(2005)185]

In spherical nuclei L= 2 and L= 4 transitions can also be identified using DWBA analysis,
But in deformed nuclei the angular distributions for L= 0 are often distorted by multistep excitations which can be described by couple-channels calculations.

For an odd-mass target the unpaired nucleon behaves as a ‘spectator’, and the level in the final nucleus with the same configuration as the target ground state ahs the strong L= 0 transition.

4. Reactions with Inverse Kinematics

The nuclide considered as the target in ‘traditional’ experiments is instead the projectile.
Changes to the projectile can be studied.
Can use radioactive ion beams (RIB) from fragmentation reactions, and effectively do experiments not possible in the ‘traditional’ manner (e.g. they would require targets too short-lived to be practical).

Some experiments reported may at first appear to be in this category but are not direct single-step transfers, e.g.,

- Many experiments used on-line isotope seperators (e.g., ISOLDE at CERN) to create RIB’s, and the decays were studied with other spectroscopic techniques.

  Decay process is not a direct transfer reaction.
- Notani *et al.* {Nucl. Phys. A **746** (2004) 113c} at RIKEN studied $^{14}O(a,p)^{17}F$ resonances with an ^{14}O beam on a He gas target (important in stellar rp process breakout from CNO cycle).

  Resonance indicated compound nuclear reaction.
- Ibbotson *et al.* {Phys. Rev. Lett. 80 (1998) 2081} used beams of $^{32,34,36,38}Si$ on a Au target at NSCL and measured gamma’s in coincidence with forward emitted ions for Coulomb excitation studies of the projectiles.

  Coulomb excitation is not a transfer reaction.

These are all useful experiments which yield information not otherwise easily accessible but are outside the scope of this talk.

We shall next consider an elegant technique developed in recent years which does satisfy the conditions for direct single-step transfer, using inverse kinematics, and which can yield good spectroscopic strengths. Method developed largely from techniques used to study halo nuclei, e.g., ^{11}Li.

4. Reactions with Inverse Kinematics *cont.*

Very sophisticated and selective experiments using RIB's done at NSCL in Michigan.

Primary cyclotron beam hits a target, and fragmentation reactions produce a variety of radioactive species. Ion beams of the desired isotope are purified by a highly selective fragment separator, and used as the beam fro the reactions of interest on a second target.

The target is surrounded by a position-sensitive array of NaI(Tl) detectors, which detect gamma rays in coincidence with the reaction products selected on the focal plane of the spectrograph.

The x/y position-sensitive focal plane detector permits particle identification and trajectory reconstruction. Momentum resolution is $\Delta p/p=0.025\%$ and momentum acceptance range is $\pm 2.5\%$.

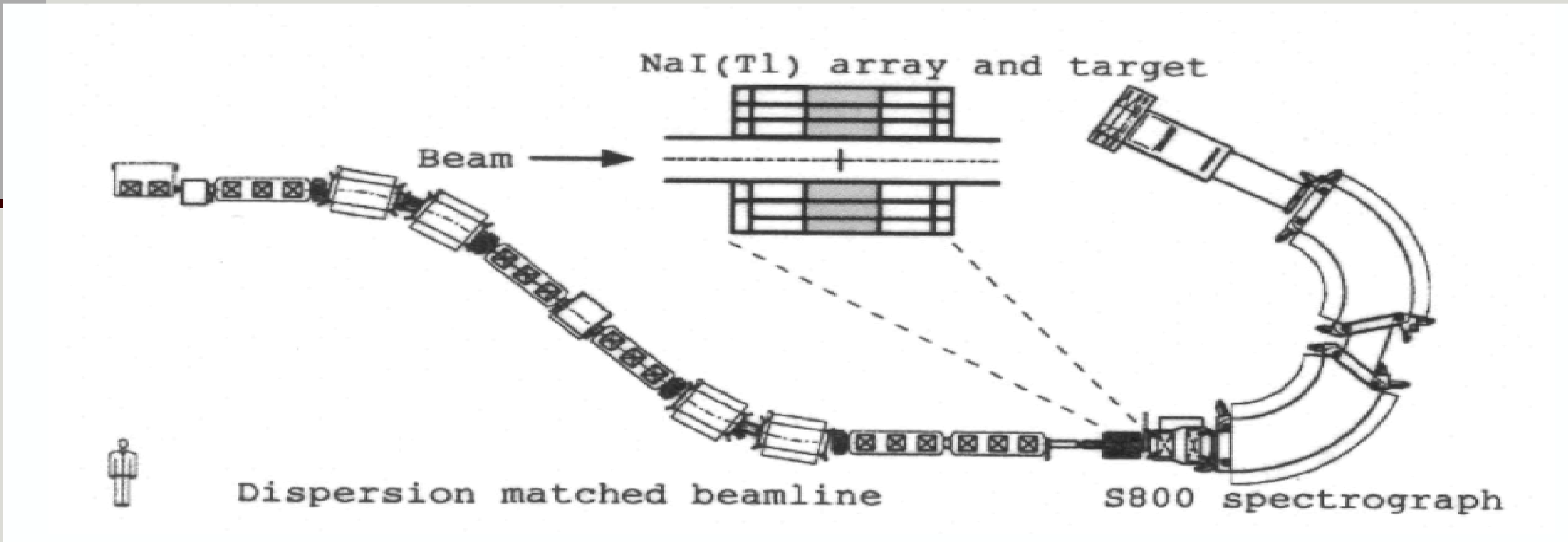

4. Reactions with Inverse Kinematics *cont.*

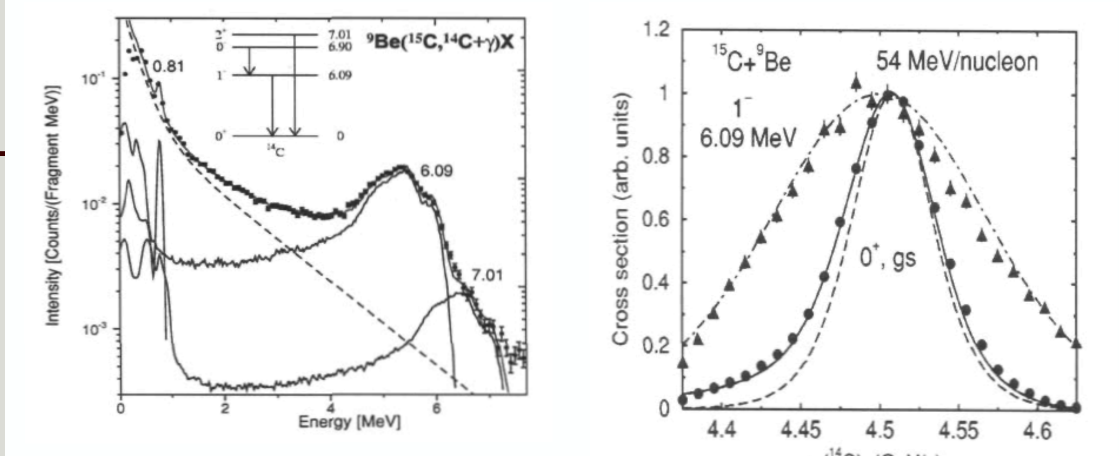

[Tostevin *et al.* Phys. Rev. C66(2002)024607]

Results from a ^{9}Be(^{15}C,^{14}C) experiment studying transitions to ^{14}C levels (^{9}Be is a good target – no bound excited states).

Left: gamma-spectrum in coincidence with ^{14}C ions on focal plane.

Right: ^{14}C ion momentum spectrum in focal place detector. Data for the 1- level at 6.09 MeV are from coincidences with the 6.09 MeV gammas. Those for ground state are NOT in coincidence with gamma's.

N.B.: Dispersion compensation of magnets in entire system causes observed momentum spread to be essentially the momentum in the ^{15}C projectile of the 'knocked-out' neutron.

Curves are theoretical predictions for l =0 and l =1 neutron removal in these knock-out or breakup reactions, and are clearly distinctive enough to determine the l-transfer. Absolute transition intensities are found to give reliable spectroscopic factors.

4. Reactions with Inverse Kinematics *cont.*

These are knock-out or breakup reactions, not 'transfers', and DWBA calculations are not sufficiently accurate.

Eikonal methods can be used, and give the dashed curves shown. The solid curve shown for the ground state transition is from a coupled discretised continuum channels (CCDC) method.

Such experiments useful for determining the spatial distributions of nucleon single-particle orbitals in the nucleus (e.g. an incentive for development of technique was to study neutron halo effects).

Method has also been used for single-proton-transfer and two-proton transfer reactions. e.g.:

^{9}Be(^{27}P,^{26}Si) by Navin et al. [Phys. Rev. Lett. **81** (1998) 5089], and

^{9}Be(^{28}Mg,^{26}Ne) Bazin et al. [Phys. Rev. Lett. **91** (2003) 012501].

See review article by P.G. Hansen and J.A. Tostevin, Annu. Rev. Nucl. Part. Sci. **53** (2003) 219.

It is clear that l –transfers and strengths can only be reliably determined for cases where the level spacing is large, and therefore this method is best suited for light nuclei (and cases near the drip lines, where there may be only one bound state).

However, these are very important cases to study, because many of them have astrophysical significance and are not accessible with other techniques. Also, the study of nuclear physics effects far from the lines of stability is of interest.

------------------- end of D.G. Burke presentation --------------

Coulomb excitation with particle and/or gamma detection

- $J\pi$: determined if the excitation probability agrees with that calculated by Alder (1960Al23).
- low energy Coulomb excitation is predominantly E2
- $B(E\lambda)$ – for excitation (*i.e.,* $B(E\lambda)\uparrow$)
- E2 (or M1) matrix element should be given in comments
- Deduce $B(E\lambda)$ **=** $|\langle M(E\lambda)\rangle|^2 / (2J_i+1)$ where J_i is initial spin.
- $B(E\lambda; i\rightarrow f)\uparrow = B(E\lambda: f\rightarrow i)\downarrow \times (2J_f+1)/(2J_i+1))$
- In strongly-deformed region, a cascade of E2 transitions with enhanced transition probabilities ($B(E2)_W > 10$): evidence for a rotational band and for the sequence of $J\pi$ values, if $J\pi$ of one level is known independently.
- Deduce $T_{1/2}$ from $B(E\lambda)$ and adopted γ-branching ratios when possible.
- Mixing ratio can sometimes be extracted from M1, E2 matrix elements. Refer to Reorientation method for quadrupole moment.

Thermal and resonance (ARC) neutron capture studies: (n,γ) E=thermal, (n,γ) E=res

- Use separate datasets for thermal and resonance n-capture data.
- Primary and secondary transitions usually appear in the same dataset even if their intensities require different normalizations.
- The Jπ of the thermal neutron capture state(s) is Jπ(target)±1/2 (*i.e.*, s-wave capture is assumed).
- In thermal neutron capture, the multipolarity of a primary γ is E1 or M1 for strong gamma rays; M1+E2 or E2 for weaker ones.
- For resonance n capture, it is optional to include the resonances and their properties; it is required to give the bound states fed, their interconnecting gammas and any conclusions concerning level Jπ.
- In average resonance n capture ARC), include primary and secondary gamma-ray data, and reduced intensities (which carry information on final state Jπ); final bound level energies and deduced Jπ

Nuclear Resonance Fluorescence: Pygmy dipole resonances and scissors mode excitations: current interest

- (γ,γ) , (γ,γ'), (pol γ,γ') measurements with bremsstrahlung spectrum; low momentum transfer so mainly E1 and M1, but some E2 excitation.
- γ spectrum measured; areas of γ peaks at Ex_0 and Ex_1, combined with knowledge of $N\gamma(Ex_0)$, yields scattering cross sections from which width and branching information may be obtained.
- γ asymmetry differentiates D and Q excitation
- γ linear polarization differentiates M and E
- Integrated) scattering cross section I_s (eV b) is often given as:
- $I_s = g(\Gamma\gamma_0\Gamma\gamma_f /\Gamma) (\pi\hbar c/E\gamma)^2$, where $g= (2J+1)/(2J_0+1)$, $E\gamma$ in MeV
- where J_0 is g.s. spin, J is spin of excited level, Γ is its total width and Γ_0, Γ_f partial decay widths for γ decay to the g.s. and the final state f, respectively; for elastic scattering, $\Gamma\gamma_0 = \Gamma\gamma_f = \Gamma$. From $g(\Gamma\gamma_0{}^2 /\Gamma)$ and $\Gamma\gamma_0/ \Gamma$ (or $I\gamma_0/\Sigma I(\gamma)$), deduce Γ or level half-life. $T_{1/2}$ (ps)= 0.456 $/\Gamma$ (meV)
- $B(E1)\uparrow = 0.955(g\Gamma\gamma_0/E\gamma^3)$ $[10^{-5}e^2b]$.
- $B(M1)\uparrow = 0.0864(g\Gamma\gamma_0/E\gamma^3)$ $[\mu^2_N]$

XUNDL Database

eXperimental Unevaluated Nuclear Data List

Available on: http://www.nndc.bnl.gov/xundl/

http://www.nndc.bnl.gov/XUNDL/

XUNDL

- eXperimental Unevaluated Nuclear Data List

Compiled (in ENSDF format) Nuclear Structure data from reactions and radioactive decays from current papers in PRL, PL-B, Nature, PR-C, NP-A, EPJ-A, JP-G, and several others. In general, information is provided from a single journal article, or from a set of follow-up articles by the same experimental group. About 85% information is from PRC and PRL.

Topics: levels and gamma rays from reactions and decays, level lifetimes, spins, rotational and quasi-rotational bands, B(E2), moments, nuclear radius, etc. For a good evaluation, compilation of all available data on a topic in a correct, complete and consistent manner is a must.

Started in December 1998 at McMaster University in response to recommendations of an advisory panel for nuclear data program set up by Office of Science, DOE in 1996, that high-spin data in ENSDF database were lagging far behind. Until 2004, compilations were for high-spin papers only. Since then all experimental structure papers are compiled.

XUNDL: Participants

- Bulk (~80%) of the compilations are done at McMaster; network coordination at McMaster.
- Since April 2008, Dr. Filip Kondev (ANL): NP-A, PL-B, JP-G
- Since April 2009, Dr. John Kelley (TUNL): A=2-20
- Since Oct 2013: Dr. C. Nesaraja (ORNL), Dr. S. Basunia (LBNL)
- Drs. S. Lalkovski (Sofia), K. Abusaleem (Jordan), A. Chakraborty (Visva Bharati), D. Symochko (Darmstadt)
- Database management: Dr. Jagdish Tuli at NNDC, BNL

- Most papers compiled within a month or earlier of their appearance in journal web pages. Many 2014 papers in PRC and PRL are already in the database.

XUNDL: Purpose and Scope

- Provides prompt internet access to nuclear structure data in current publications through on-line retrieval system at NNDC, BNL; and through RADWARE level-scheme database at ORNL.
- Complements ENSDF database, where data for some of the nuclides may be several years old and outdated.
- Serves as a repository of relevant data details which for one reason or another do not appear in publications. Some authors send data tables and other details for some of their papers in PRL/PRC to include data details only in XUNDL database.
- Example: e-mail of Jan 13, 2014 from Professor Sean Freeman at Univ. of Manchester, UK

XUNDL: Researchers' unsolicited response

From: Sean Freeman <sean.freeman@manchester.ac.uk>
Subject: Cross section data for (a,t) and (3He,d) reactions on isotopes of Sn
Date: Mon, 13 Jan 2014 11:42:32 +0000
To: "hispin@univmail.cis.mcmaster.ca" <hispin@univmail.cis.mcmaster.ca>, Balraj Singh <ndgroup@univmail.cis.mcmaster.ca>
Cc: AJ Mitchell <ajmitchell5@gmail.com>

Dear Balraj:

Happy New Year!

I'm attaching here a pdf document containing data tables of reaction cross sections for the (a,t) and (3He,d) reactions on stable isotopes of Sn, along with a short description of the experiment from which they were deduced, which we hope would be of use for the XUNDL data base.

These data were taken from an experiment performed around three years ago that were analysed by one of my PhD students, AJ Mitchell. They were taken to make some checks on an earlier data set that had been previously published. Embarrassingly, this highlighted an issue with that previous data and we corrected this with an erratum (http://prl.aps.org/pdf/PRL/v110/i16/e169901).

We would like to make the data available to any other interested parties, now or in the future, by making the data available via XUNDL. As you know we have been trying to do this regularly with our work since there is often not the space to publish every single piece of numeral data in journal publications. This is particularly acute when it is used as part of an erratum.

With very best wishes

Sean

****

Prof Sean J Freeman

Nuclear Physics Research Group

School of Physics and Astronomy
the University of Manchester
Oxford Road, Manchester, M13 9PL
United Kingdom

XUNDL: Researchers' submitted paper to XUNDL

Submission to XUNDL: data from the $^{112-124}$Sn(α,t)$^{113-125}$Sb and $^{112-124}$Sn(^{3}He,d)$^{113-125}$Sb reactions

A. J. Mitchell,[1] S. J. Freeman,[1] J. P. Schiffer,[2] J. A. Clark,[2] C. M. Deibel,[2, 3], C. R. Hoffman,[2] A. M. Howard,[1], B. P. Kay,[2] P. D. Parker,[4] D. K. Sharp,[1] and J. S. Thomas[1]

[1]*School of Physics and Astronomy, University of Manchester M13 9PL, United Kingdom*
[2]*Physics Division, Argonne National Laboratory, Argonne, Illinois 60439, USA*
[3]*Joint Institute for Nuclear Astrophysics, Michigan State University, East Lansing, Michigan 48824, USA*
[4]*A. W. Wright Nuclear Structure Laboratory, Yale University, New Haven, Connecticut 06520, USA*

(Dated: January 14, 2014)

NSR key-number (2014MiZZ) was assigned and key-words written.

A total of 7 datasets were prepared and entered in XUNDL.

Only place for public archival of such data!

Someday, these data may get included in ENSDF database.

XUNDL: Purpose and Scope

- Not limited to regular journal publications only.
- At the request of researchers, unpublished data for completed studies or from preprints can also be included. Papers dealing only with analysis of experimental data can also be included.
- It is called “Unevaluated”, yet each paper goes through a critical compilation with partial evaluation within the context of the paper, and problems identified and resolved. However, no comparisons are made with papers from other labs on the same topic.

XUNDL

- Identify data-related problems or lack of detailed data in a paper. If so, consult author(s) for clarification or obtaining data details. Extensive communications with authors have taken place with about 600 of these since 1999. Several errata have appeared as a result of these.
- Browse database by nuclide, mass number, index. Also by article through NSR database.
- At McMaster, most draft datasets are prepared by one or two undergraduate (first and second-year Physics) students, working full-time in summer and part-time during semesters. They also get an opportunity to participate in experimental work in nuclear astrophysics in other major accelerator labs. Students get training in basic nuclear physics, use of ENSDF, NSR databases; and the computer codes related to ENSDF work.

The XUNDL Data Format: ENSDF

2014Mo02: PRC 89, 014324 (Jan 2014)

```
215PO     215BI B- DECAY:7.6 M:XUNDL-3  2014MO02                            201403
215PO c   Compiled (unevaluated) dataset from 2014Mo02:
215PO2c   Phys Rev C 89, 014324 (2014)
215PO3c   Compiled by B. Singh (McMaster), March 5, 2014
215PO c   2014Mo02 state that proposed decay scheme is tentative
215PO c   {+215}Bi was produced by projectile fragmentation using E({+238}U)=1
215PO2c   GeV/nucleon beam provided by the UNILAC-SIS accelerator facilities at
215PO3c   GSI with an intensity of 1.5|*10{+9} ions/spill (a repetition of 3 s
215PO4c   and an extraction time of 1 s). The reaction products were separated
215PO5c   and identified in the magnetic spectrometer Fragment Separator (FRS).
215PO6c   Separation of {+215}Bi nuclei is based on B|r-|DE-B|r scheme.
215PO7c   At the focal plane, the recoils were slowed down in an Al degrader
215PO8c   and implanted in a composite DSSSD detector system comprising of 3
215PO9c   layers, each with 3 DSSSD pads with 16x16 pixels, and dimensions of
215POAc   5x5 cm{+2} and 1 mm thick.  The DSSSD detectors were surrounded by
215POBc   the RISING |g-ray spectrometer comprised of 105 HPGe crystals
215POCc   arranged clusters of seven elements. Measured E|g, I|g, |g|g-coin,
215PODc   |b-|g-t coin in coincidence with implanted recoils.
215PO cG  E$Uncertainty is within the intrinsic FWHM of the RISING array
215PO cL  E$From E|g data, assuming 1 keV uncertainty for each E|g
215PO cL  J$From 2014Mo02
215BI  P  0.0          (9/2-)          7.6 M     2                 2189    15
215BI cP  T$From Adopted Levels of {+215}Bi in ENSDF database
215BI cP  QP$From 2012Wa38
215PO  N                             1
215PO cN  BR$%|b{+-}=100
215PO PN                                                                  5
215PO  L  0              9/2+
215PO  L  271        1    7/2+
215PO  G  271          6.8    10                                          C
215PO  L  293        1  (11/2)+
215PO  G  293          100    8                                           C
215PO  L  402       1    (5/2+)
215PO  G  402           1.4   5
215PO  L  517        1  (7/2+,9/2+)
215PO  G  517           4.7   9                                           C
215PO  L  835        1
215PO  G  564           1.5   5
215PO  G  835           1.5   6
215PO  L  877       1
215PO  G  877           1.3   5
215PO  L  1009      1
215PO  G  1009          0.9   5
215PO  L  1077      1
215PO  G   785          0.6   4                                           C
215PO  G   805          0.8   4                                           C
215PO  G  1075          2.7   8                                             ?
215PO  L  1150      1
215PO  G  1150          1.8   7
215PO  L  1293      1
215PO  G   776          2.0   7                                           C
215PO  G  1022          0.7   4                                           C
215PO  L  1398      1
215PO  G  1105          2.2   8
215PO  G  1399          0.3   3
```

XUNDL: HTML viewer

Download: XU_B20A1379B25E2754E48CFBBD5DE47A53_1.ens **View:** Levels: PostScript level schemes in the Nuclear Data Sheets style

^{215}Po

^{215}Bi β^- Decay: 7.6 M:xundl-3 2014Mo02

201403

^{215}Bi Parent: E_x=0.0; J^π=(9/2-); $T_{1/2}$=7.6 min *2*; $Q_{g.s.\to g.s.}$=2189 *15*; %β^-=100

$T_{1/2}$: From Adopted Levels of ^{215}Bi in ENSDF database.

$Q_{g.s.\to g.s.}$: From 2012Wa38.

Compiled (unevaluated) dataset from 2014Mo02: Phys Rev C 89, 014324 (2014) Compiled by B. Singh (McMaster), March 5, 2014.

2014Mo02 state that proposed decay scheme is tentative.

^{215}Bi was produced by projectile fragmentation using E(^{238}U)=1 GeV/nucleon beam provided by the UNILAC-SIS accelerator facilities at GSI with an intensity of 1.5×10^9 ions/spill (a repetition of 3 s and an extraction time of 1 s). The reaction products were separated and identified in the magnetic spectrometer Fragment Separator (FRS). Separation of ^{215}Bi nuclei is based on Bρ-ΔE-Bρ scheme. At the focal plane, the recoils were slowed down in an Al degrader and implanted in a composite DSSSD detector system comprising of 3 layers, each with 3 DSSSD pads with 16x16 pixels, and dimensions of 5x5 cm^2 and 1 mm thick. The DSSSD detectors were surrounded by the RISING γ-ray spectrometer comprised of 105 HPGe crystals arranged clusters of seven elements. Measured Eγ, Iγ, γγ-coin, β-γ-t coin in coincidence with implanted recoils.

^{215}Po levels

E_{level}#	J^π@	E_{level}#	J^π@	E_{level}#	J^π@	E_{level}#	J^π@
0.0	9/2+	402 *1*	(5/2+)	877 *1*		1150 *1*	
271 *1*	7/2+	517 *1*	(7/2+,9/2+)	1009 *1*		1293 *1*	
293 *1*	(11/2)+	835 *1*		1077 *1*		1398 *1*	

From Eγ data, assuming 1 keV uncertainty for each Eγ.
@From 2014Mo02.

γ(^{215}Po)

Branching Ratio: %β^-=100.

E_γ#	E_{level}	I_γ	E_γ#	E_{level}	I_γ	E_γ#	E_{level}	I_γ
271	271	6.8 *10*	785	1077	0.6 *4*	1075@	1077	2.7 *8*
293	293	100 *8*	805	1077	0.8 *4*	1105	1398	2.2 *8*
402	402	1.4 *5*	835	835	1.5 *6*	1150	1150	1.8 *7*
517	517	4.7 *9*	877	877	1.3 *5*	1399	1398	0.3 *3*
564	835	1.5 *5*	1009	1009	0.9 *5*			
776	1293	2.0 *7*	1022	1293	0.7 *4*			

Uncertainty is within the intrinsic FWHM of the RISING array.
@Placement in the level scheme is uncertain.

XUNDL HTML Viewer: level scheme drawing

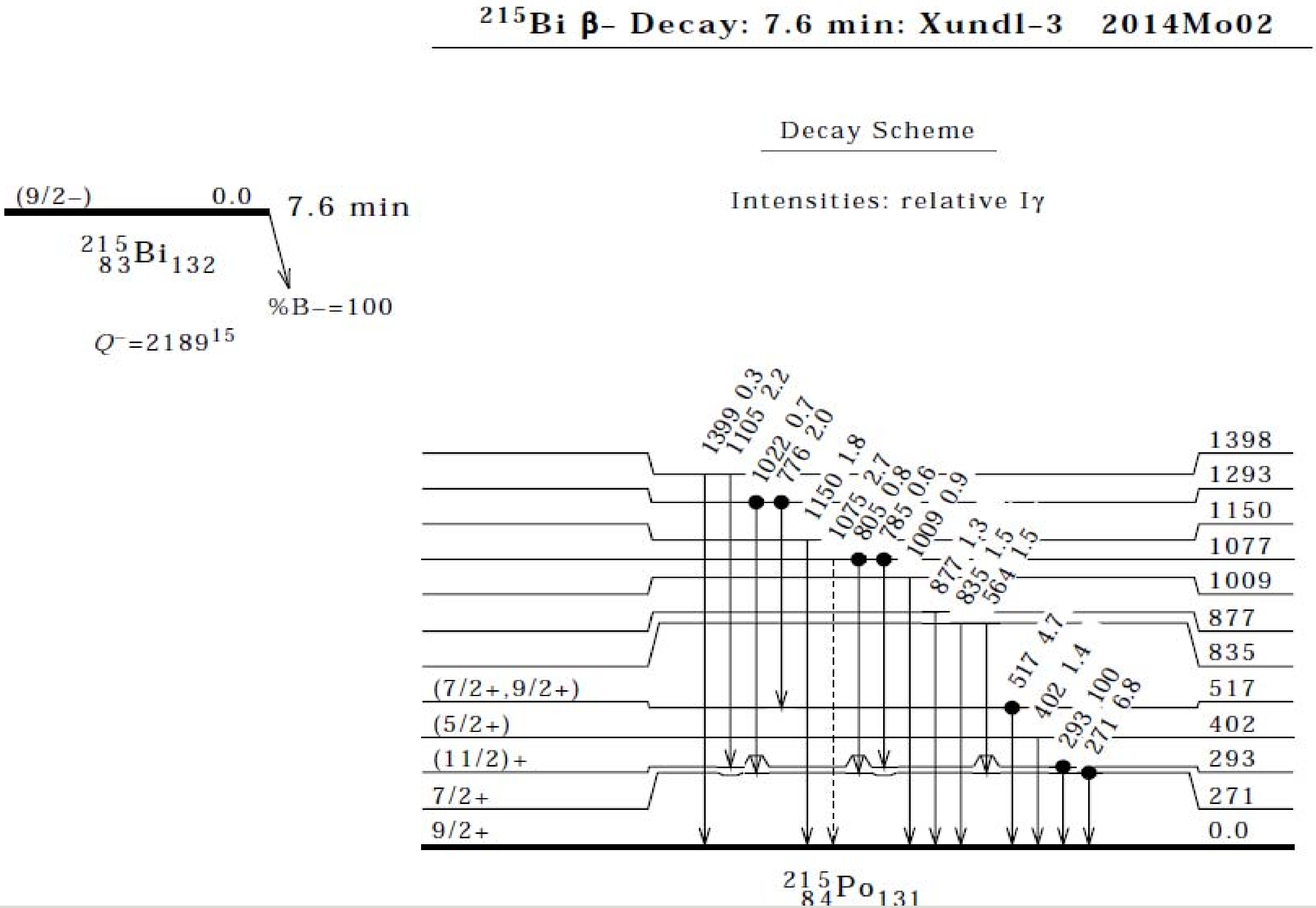

Example: serious correction to level scheme

2012HE17： PRC 86, 047302 (Oct 2012)

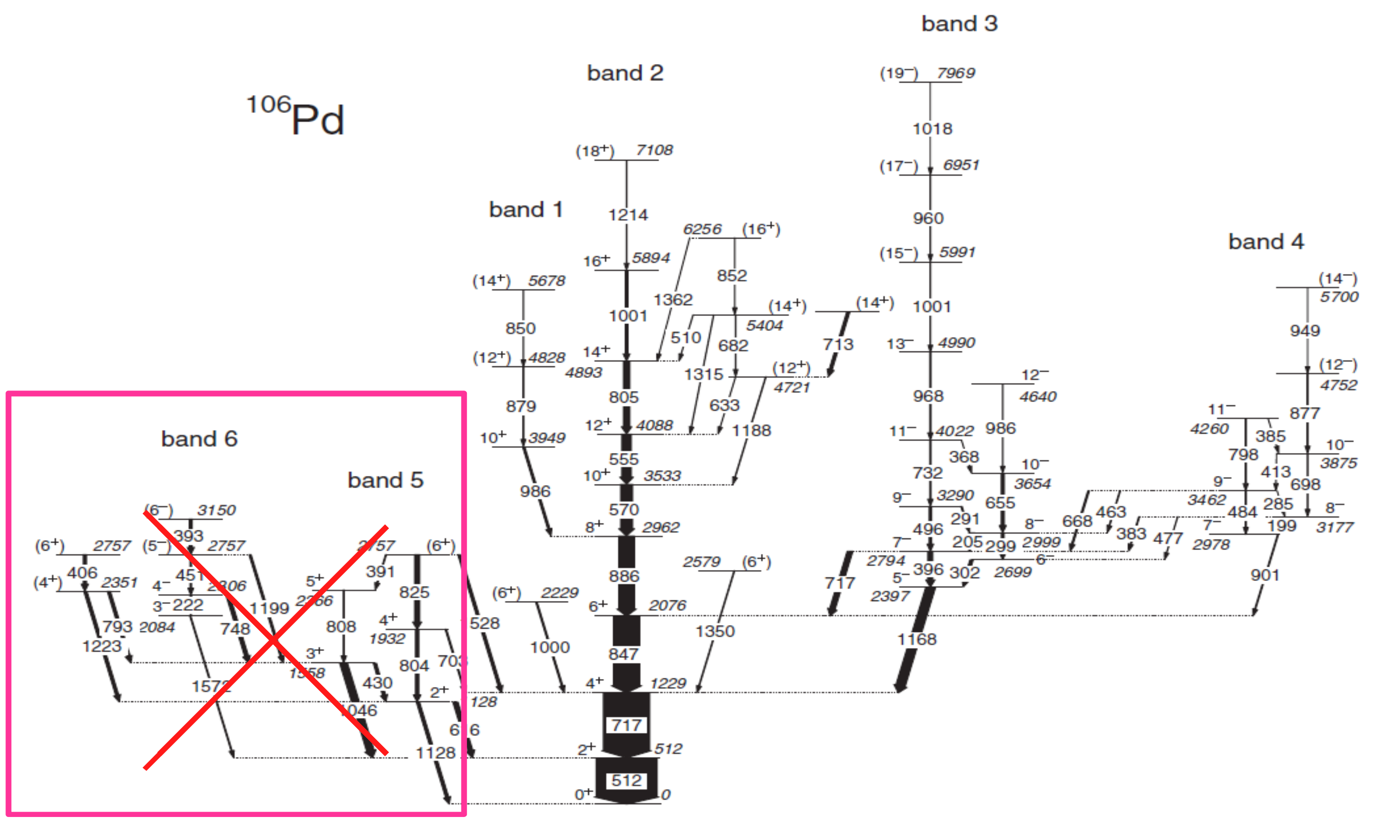

FIG. 1. Deduced new level scheme of ^{106}Pd from the present experiment. The γ energies are in keV. The widths of the arrows are proportional to the intensities of the transitions.

2012He17: PRC 86, 047302

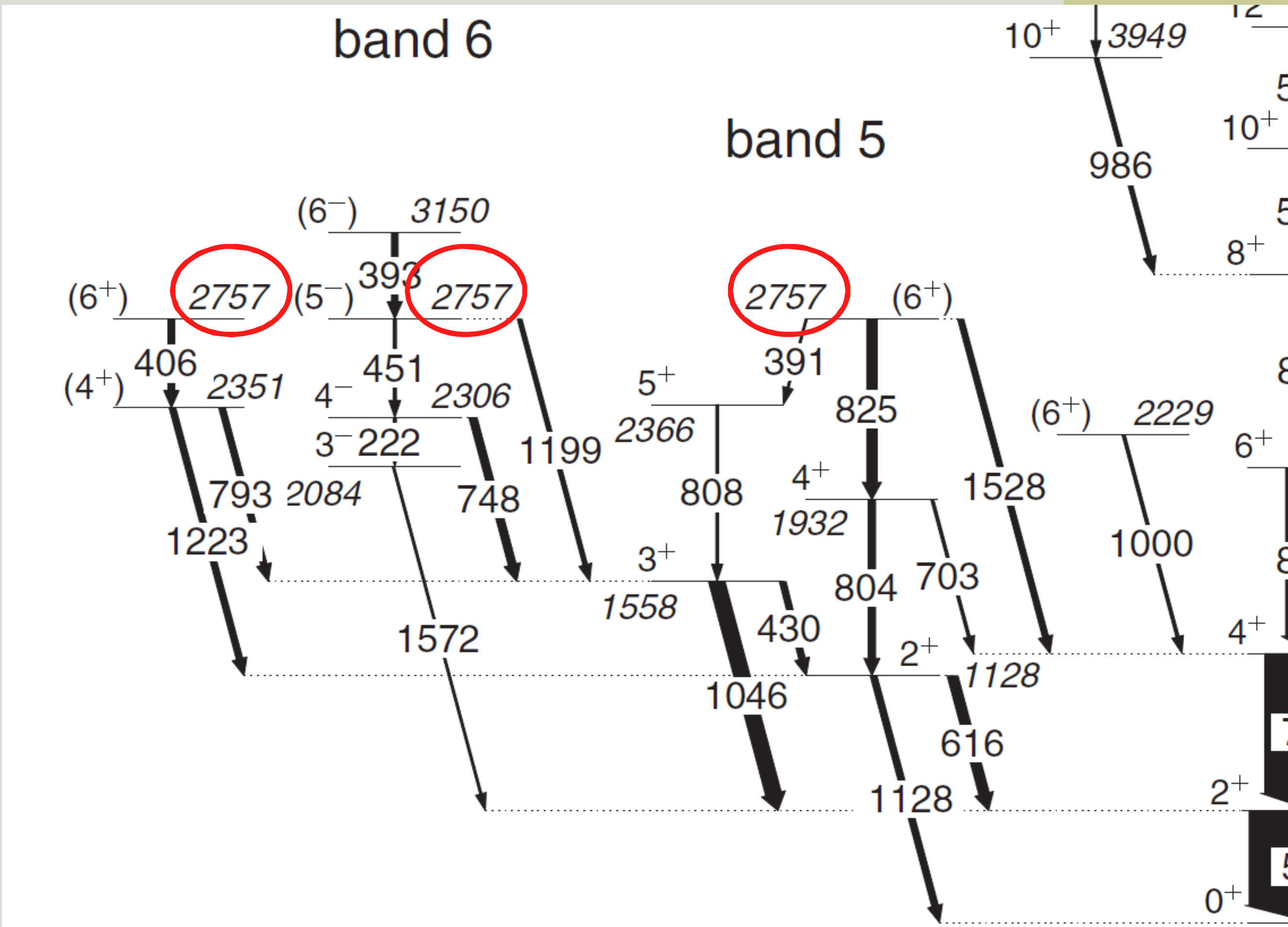

of the shape of ^{106}Pd, and one can see in Fig. 3 that the experimental alignments have nearly constant alignment after band crossing. One should note that the band crossing happens around the same spin point as the inflection of E-GOS curve. The transition from vibrational mode to collective mode could therefore be a result of the band crossing.

The low-lying cascade, which is labeled with band 5 in Fig. 1, established on the second 2^+ state is assigned as the γ-vibrational band since this kind of collective motion is a common feature in even-even Pd isotopic nuclei [14,15]. Recently, such a structure has been identified also in ^{104}Pd [16], and it was interpreted as a quasi-γ band associated with γ-soft deformation. In order to further understand the shape of ^{106}Pd, the staggering signature defined as [17]

$$S(I, I-1, I-2) = \frac{E(I) + E(I-2) - 2E(I-1)}{E(2_1^+)} \quad (1)$$

has been calculated. It is a good indicator for distinguishing between γ-soft and γ-rigid potentials. When the staggering gives positive values, the potential is triaxial rigid; when it is negative it is γ-soft. The experimental odd-even spin energy staggering deduced for band 5 is displayed in Fig. 5 together with the values extracted for ^{104}Ru [18]. It is clear that the even spin has negative values, while the odd spin has positive values, which is the same as occurs in ^{104}Pd [16]. Thereby, one can rule out the γ-rigid potential scenario for ^{106}Pd. On the other hand, cranked Woods-Saxon-Strutinsky calculations have also been performed by means of total Routhian surface (TRS) methods in a three-dimensional deformation space (β_2, β_4, γ) [19,20]. At a given frequency, the deformation of a state is determined by minimizing the resulting total Routhian surfaces. Figure 6(a) displays a prolate shape for the vacuum configuration of ^{106}Pd nuclei. The minimum is located at $\gamma \approx 0$, but with large softness in the γ direction. This statement is in agreement with the results of the staggering signature calculation. In addition, the $E2$ transitions in band 5 remains nearly constant in energy. All this combined evidence above give a confident assignment to band 5 as a γ-vibrational band. It should be mentioned that the second 2^+ state was also interpreted as a two-phonon triplet state in Ref. [21]. This interesting phenomenon provides a challenge to theory and deserves further investigation by the nuclear physics community.

The bandhead energy of band 6 has a value similar to that of band 3. It has been pointed out by using Hartree-Fock-Bogoliubov calculations [18] that the lowest two-proton and two-neutron states are expected to have similar excitation energy. The lowest two-proton quasiparticle state is the coupling between $\pi\ p_{1/2}$ and $\pi\ g_{9/2}$. Indeed, similar structure has been found in the neighboring isotopic nuclei ^{104}Pd [16]. Thereby, the configuration is assigned as proton $g_{9/2} \otimes p_{1/2}$.

In conclusion, the high spin states of the ^{106}Pd nucleus have been measured and the level scheme has been updated considerably. Band 2 has good rotational character after an alignment built on a pair of $h_{11/2}$ neutrons. Bands 3 and 4 could make a pseduospin doublet bands. Band 5 has γ-vibrational character. The newly constructed band 6 possibly originates from two-quasiproton excitation.

2012HE17: PRC-Oct 12

Another example: Hg-184
Minor but significant correction in paper and ENSDF: 2014Ga04: PRC 89, 024307

	I^{π} ($\hbar$)	E_{γ} (keV)	b.f.	τ_{av} (ps)	τ_{prev} (ps)	$B(E2)\downarrow$ (W.u.)	$\lvert Q_t \rvert$ (e b)
^{184}Hg	2_1^+	366.8	1	35.7(15)	30(7)	52(2)	4.04(8)
	4_1^+	287.0	0.959(4)	30.2(10)	32.8(34)	191(6)	6.46(11)
	6_1^+	340.1	1	8.7(4)	8.1(31)	308(15)	7.81(19)
	8_1^+	418.3	1	3.19(14)	$2.9^{+1.1}_{-1.6}$	309(13)	7.65(17)
	9_3	329.1	0.65(16)	12.1(8)		169(40)	5.6(7)

Another example

- 2014Ga04: PRC 89, 024307 (Feb 11, 2014): level lifetimes by DSAM
- 2450-keV level, J=9, 329.1-keV most intense γ: measured τ=12.1(8) ps
  B(E2)(W.u)=169(40) , Q(transition)=5.6(7), used BR=0.65(16) from ENSDF

- Question: why uncertainty in BR is so large, if 329γ is most intense transition?
- Answer: in ENSDF Adopted dataset: typo in BR: 100(17) should be 100.0(17)
- Query e-mail sent to first author: Feb 11, 2014.
- Prompt response from author: Feb 12, 2014 with
  Revised B(E2)(W.u.)=169(11), Q(transition)=5.62(19)
- Correction of typo in ENSDF sent to Dr. Tuli at NNDC, BNL: Feb 12, 2014
- Dataset in XUNDL database; and correction in ENSDF appear: Feb 15, 2014.

THANK YOU